Tonic and Phasic Tetrodotoxin Block of Sodium Channels with Point Mutations in the Outer Pore Region

Anna Boccaccio, Oscar Moran, Keiji Imoto,[#] and Franco Conti
Istituto di Cibernetica e Biofisica, CNR, I-16149 Genova, Italy [#]National Institute for Physiological Sciences, Okazaki 444, Japan

ABSTRACT Tonic and use-dependent block by tetrodotoxin (TTX) has been studied in cRNA-injected *Xenopus* oocytes expressing mutants W386Y, E945Q, D1426K, and D1717Q, of the outer-pore region of the rat brain IIA α-subunit of sodium channels. The various phenotypes are tonically half-blocked at TTX concentrations, $IC_{50}^{(t)}$, that span a range of more than three orders of magnitude, from 4 nM in mutant D1426K to 11 μM in mutant D1717Q. When stimulated with repetitive depolarizing pulses at saturating frequencies, all channels showed a monoexponential increase in their TTX-binding affinity with time constants that span an equally wide range of values ([TTX] $\approx IC_{50}^{(t)}$, from ~60 s for D1426K to ~30 ms for D1717Q) and are in most phenotypes roughly inversely proportional to $IC_{50}^{(t)}$. In contrast, all phenotypes show the same approximately threefold increase in their TTX affinity under stimulation. The invariance of the free-energy difference between tonic and phasic configurations of the toxin-receptor complex, together with the extreme variability of phasic block kinetics, is fully consistent with the trapped-ion mechanism of use dependence suggested by Salgado et al. (1986) and developed by Conti et al. (1996). Using this model, we estimated for each phenotype both the second-order association rate constant, k_{on}, and the first-order dissociation rate constant, k_{off}, for TTX binding. Except for mutant E945Q, all phenotypes have roughly the same value of $k_{on} \approx 2\ \mu M^{-1}\ s^{-1}$ and owe their large differences in $IC_{50}^{(t)}$ to different k_{off} values. However, a 60-fold reduction in k_{on} is the main determinant of the low TTX sensitivity of mutant E945Q. This suggests that the carboxyl group of E945 occupies a much more external position in the pore vestibule than that of the homologous residue D1717.

INTRODUCTION

The puffer fish poison tetrodotoxin (TTX) is a very potent blocker of the voltage-gated sodium channel that can suppress the action potential of nerve, muscle, and most excitable cells at nanomolar concentrations (Narahashi et al., 1964; Narahashi, 1974; Kao, 1986). Like the other guanidinium toxin saxitoxin (STX), TTX selectively and reversibly blocks the sodium currents acting from the extracellular side. Evidence suggests that TTX and STX bind as a plug to the extracellular mouth of the channel, blocking the flow of ions through the pore (Hille, 1975, 1992). By use of the sensitivity to TTX and STX as an assay, several residues of the rat brain α-subunit (rBIIA) have been mapped by site-directed mutagenesis to the pore region of the sodium channel (Noda et al., 1989; Terlau et al., 1991; Satin et al., 1992; Kontis and Goldin, 1993). Many of these residues also affect the pore conductance, and two important rings of polar residues from the four homologous repeats of the channel polypeptide were identified: an outer ring that is most influential for toxin binding and an inner ring consisting of determinants of pore permeability and selectivity (Pusch et al., 1991; Terlau et al., 1991; Heinemann et al., 1992). These data also encouraged the early proposal of speculative computer-aided molecular models of the sodium pore (Lipkind and Fozzard, 1994).

Use dependence (UD) is a common feature of the block of sodium channels by TTX (Baer et al., 1976; Cohen et al., 1981; Carmeliet, 1987; Lönnendonker, 1989, 1991a,b; Eickhorn et al., 1990; Patton and Goldin, 1991; Conti et al., 1996) and by STX (Salgado et al., 1986; Lönnendonker, 1989, 1991a,b; Satin et al., 1992, 1994; Makielski et al., 1993). The phenomenon consists of an increase in toxin block triggered by depolarizing pulses. To account for the UD of STX block of sodium currents in crayfish giant axons, Salgado et al. (1986) proposed that a large fraction of the tonic block is due to toxins that have trapped a repelling cation while plugging the pore, and that the efficiency of the block increases when the opening of the cytoplasmic gates allows the escape of the cation to the intracellular medium. By elaborating a detailed kinetic scheme according to this idea, Conti et al. (1996) have shown that such a "trapped-ion" model quantitatively accounts for all of the measurable properties of the tonic and phasic TTX block of rBIIA channels expressed in frog oocytes. The model predicts that the size of the effect depends on the repulsion energy between a bound TTX and a trapped cation, whereas the kinetics is mainly governed by the rate constants of second-order association and first-order dissociation of the TTX-receptor complex.

Single point mutations in the pore region affect to various degrees the sensitivity of the sodium channel to guanidinium toxins and may increase the half-block concentration ($IC_{50}^{(t)}$) of TTX and STX by several orders of magnitude (Terlau et al., 1991). A more detailed description of these effects in terms of the second-order association and first-order dissociation rate constants can unravel features of the free-energy profile of the toxin binding reaction relevant to

Received for publication 4 December 1998 and in final form 12 April 1999.

Address reprint requests to Dr. Franco Conti, Istituto di Cibernetica e Biofisica, Consiglio Nazionale delle Ricerche, Via De Marini 6, I-16149 Genova, Italy. Tel.: +39-010-6475-592; Fax: +39-010-6475-500; E-mail: conti@barolo.icb.ge.cnr.it.

0006-3495/99/07/229/12 $2.00

the modeling of the molecular architecture of the outer sodium pore. We report here this type of study for the channels expressed in oocytes by four mutants of the rBIIA α-subunit: W386Y, E945Q, D1426K, and D1717Q. Two of the mutations (E945Q of repeat II and D1717Q of repeat IV) are at positions assigned by Terlau et al. (1991) to the outer ring of strongly TTX-sensitive residues, whereas W386Y and D1426K are one position below and one above the residues contributed to this ring by repeats I and III. Despite their dramatic differences in toxin sensitivity, all mutants show qualitatively similar use-dependent relaxations of TTX block that are consistent with the same trapped-ion mechanism postulated for WT channels (Conti et al., 1996) and that allow estimates of the rate constants of the TTX-binding reaction. An interesting outcome of our analysis is that the charge neutralizations in the homologous residues E945 and D1717 cause a similar large reduction of TTX sensitivity by having opposite effects on the kinetics of TTX binding: the rate of TTX association to mutant E945Q is much lower, whereas the off-binding of TTX from D1717Q is much faster, than for WT channels.

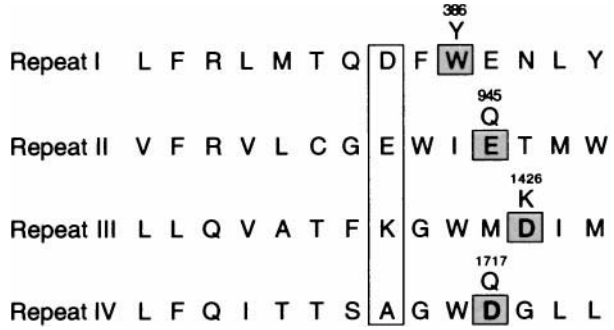

FIGURE 1 Amino acid sequence of the P segments of the four repeats of the rBIIA channel, which contribute to shaping of the pore region (single-letter amino acid code). Residues in the white box have a strong influence on the conductance and selectivity of the channel and may contribute to the filtering structure of the pore. The residues indicated by the gray boxes have significant or major effects on the binding of guanidinium toxins. The indicated mutations, selected for our study, affect the pore conductance by less than a factor of 2 (Terlau et al., 1991), presumably because they mainly influence the structure of the outer-pore vestibule and not the pore outermost cation-binding site. Mutation W386Y in the first repeat is fully conservative; mutations E945Q and D1717Q, respectively, in the second and fourth repeat, involve the neutralization of a negative charge; mutation D1426K in the third repeat involves a positive double charge increase.

MATERIALS AND METHODS

Oocyte expression

The mutations were introduced into the sodium channel type II cDNA, using the oligonucleotide-directed mutagenesis system kit (version 2; Amersham). Mutagenesis was made using smaller cDNA fragments. The mutated restriction fragments of ~500 bp were substituted for the corresponding fragments of the wild-type cDNA, to yield the mutant sodium channel type II cDNAs. The entire nucleotide sequences derived from the mutated fragments were confirmed by dideoxy terminator methods to exclude the possibility of spurious mutations. Furthermore, the mutations in the final mutant plasmids were confirmed to exclude errors in sample handling. Specific cRNAs were synthesized in vitro from their respective cDNA, using the Mmessage Mmachine kit (Ambion, Austin, TX). The four mutations (W386Y, E945Q, D1426K, D1717Q) of the pore region that we studied in this work are illustrated in Fig. 1.

Oocytes, surgically extracted from the frog *Xenopus laevis* under anesthesia, were injected with cRNA and prepared for electrophysiological recordings following standard procedures (Stühmer, 1992). In brief, after removal of the follicular cell layer by pretreatment with collagenase A (Sigma, St. Louis, MO), the oocytes were microinjected with ~50 nl of solution containing 0.25 μg/μl of cRNA. They were then incubated in Barth's solution with gentamicin (10 μg/ml) for 2–6 days before the measurements.

Solutions

The oocytes were bathed in normal frog Ringer (NFR) with the following composition (in mM): 112 NaCl, 2 $CaCl_2$, 2.5 KCl, 10 NaOH-HEPES (pH 7.2). Appropriate aliquots of freshly thawed small volumes of stock solutions (10, 100, or 500 μM) of TTX in NFR were mixed with NFR before each experiment to obtain any desired toxin concentration, [T]. All salts and TTX were purchased from Sigma. The oocytes were positioned in a recording chamber with a volume of ~120 μl. Measurements were taken in continuous perfusion of precooled solutions with a flow of 1–1.5 ml/min at a constant temperature regulated by a Peltier cell. The bath temperature, measured with a small thermistor (Ø 0.2 mm) placed in the chamber 1 mm from the oocyte, was kept between 15°C and 17°C.

Current recordings

Whole-oocyte currents were measured with a two-electrode voltage-clamp system, using a homemade high-voltage feedback amplifier. The electrode pipettes were made from borosilicate glass (Hilgenberg, Malsfeld, Germany) and filled with a solution of 3 M KCl. They had a resistance of 0.3–0.8 MΩ. Stimulation and data acquisition were controlled by a Macintosh microcomputer (Cupertino, Ca) interfaced to the voltage-clamp amplifier with a 16-bit AD/DA converter (Instrutech, Elmond, NY), using the Pulse-PulseFit software package (Heka Elektronik, Lambrecht, Germany). Currents were filtered at 5 kHz with a 4-pole low-pass Bessel filter (Ithaco, Ithaca, NY) and sampled at 20 kHz. Off-line analysis was performed with PulseFit and custom software written in the Igor environment (Wavemetrics, Lake Oswego, OR).

Subtraction of linear current responses was usually done by the Pulse program, using positive P/4 pulses from the holding potential, usually kept at −100 mV. Several experiments with the most TTX-sensitive phenotypes (WT, W386Y, and D1426K) were ended by perfusion with high concentrations of TTX that completely blocked the sodium channels, and the remaining currents could be used for a more accurate leakage subtraction. The two types of corrections usually showed significantly different pulse-onset artifacts, but were practically indistinguishable for the relevant part of the records.

Cumulative inactivation of the sodium currents during high-frequency repetitive stimulation may affect the measurement of use-dependent block. We tried to minimize these effects by using short test pulses that caused only a partial fast inactivation. In all cases cumulative inactivation during any specific stimulation protocol was measured separately under TTX-free conditions and used for off-line correction of UD effects. The correction was barely significant for the currents expressed by WT, W386Y, D1426K, and E945Q, whose maximum use-dependent block could be measured for stimulation frequencies lower than 2 Hz; it was substantial, however, in the experiments with mutant D1717Q, which has fast TTX-binding kinetics and shows large UD effects only for stimulation frequencies above 10 Hz.

Model fitting

The tonic half-blocking TTX-concentration, $IC_{50}^{(t)}$, was estimated from the resting toxin-free probability, $U_0([T])$, defined as the ratio between the

peak responses to a given pulse in stationary resting conditions at the toxin concentration [T] or at [T] = 0 and expressed as a function of [T] by

$$U_0([\mathrm{T}]) = \frac{1}{1 + [\mathrm{T}]/\mathrm{IC}_{50}^{(t)}} \quad (1)$$

The decay (UD) of the toxin-free probability during a train of saturating high-frequency stimulations, starting from stationary resting conditions at $t = 0$, was fitted by a single exponential:

$$U(t) = U_\infty + (U_0 - U_\infty)e^{-t/\tau} \quad (2)$$

and the half-concentration of stimulated TTX-block, $\mathrm{IC}_{50}^{(s)}$, was estimated from the [T] dependence of the asymptotic toxin-free probability according to

$$U_\infty([\mathrm{T}]) = \frac{1}{1 + [\mathrm{T}]/\mathrm{IC}_{50}^{(s)}} \quad (3)$$

The [T] dependence of the time constant τ was fitted by

$$\tau([\mathrm{T}]) = \frac{\tau_0}{1 + [\mathrm{T}]/\mathrm{IC}_{50}^{(s)}} \quad (4)$$

where τ_0 is the upper limit of τ for [T] = 0. The slow kinetics of TTX binding to WT and D1426K channels also allowed for these phenotypes estimates of τ_0 from the time constant of the change of unblocked currents during wash-in and wash-out experiments.

Apart from the use of different notations ($\mathrm{IC}_{50}^{(t)}$ for $1/A_t$; $\mathrm{IC}_{50}^{(s)}$ for $1/A_M$; τ_0 for $1/\nu_0$), Eqs. 1, 3, and 4 are identical to Eqs. 2, 4, and 6 of Conti et al. (1996) and are consistent with the most simple "trapped-ion" model for the use-dependent binding of TTX, described by the scheme

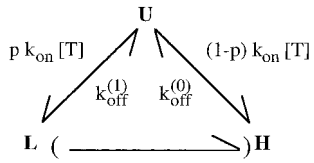

Scheme 1

where **U** represents the toxin-free (unblocked) channel, **H** represents a channel tightly binding a toxin molecule with no trapped cation, and **L** represents a channel-toxin complex that is destabilized by calcium or sodium ions trapped in the outermost site of the pore, much in the same way as K^+ destabilizes the binding of charybdotoxin to potassium channels (MacKinnon and Miller, 1988; Goldstein and Miller, 1993). **L** → **H** transitions occur almost instantaneously when the channel is open, but must proceed through relatively slow unbinding and rebinding steps if the channel is kept closed by large hyperpolarizations. The binding of TTX according to the second-order association rate constant, k_{on}, leads to state **L** or to state **H**, depending on the probability, p, that a toxin-free channel will host a cation. Because of the repulsion from the trapped cation, the rate constant of TTX dissociation from states **L**, $k_{off}^{(1)}$, is larger than that from state **H**, $k_{off}^{(0)}$. Apart from the change of notations ($k_{off}^{(0)}$ for ν_0; $k_{off}^{(1)}$ for ν; k_{on} for k_0 and k), Scheme 1 is a simplified version of more general schemes considered by Conti et al. (1996) to demonstrate the consistency of the trapped-ion model with several properties of TTX-UD in WT channels, like the dependencies on holding potential, pulse amplitude, and external Ca^{2+} concentration, which are not considered in this study. In particular, as concluded for WT from the independence of UD kinetics on Ca^{2+} concentration, it is assumed that k_{on} is independent of the state of occupancy by cations of the outermost site in the sodium pore. According to Scheme 1, the experimental quantities defined by Eqs. 1–4 are directly related to the model parameters according to

$$k_{off}^{(0)} = \frac{1}{\tau_0} \quad (5)$$

$$k_{on} = \frac{1}{\tau_0 \cdot \mathrm{IC}_{50}^{(s)}} \quad (6)$$

$$B_i = p^*\left(1 - \frac{k_{off}^{(0)}}{k_{off}^{(1)}}\right) = 1 - \frac{\mathrm{IC}_{50}^{(s)}}{\mathrm{IC}_{50}^{(t)}} \quad (7)$$

The parameter B_i defined by the last equation represents the effective tonic inhibition of TTX binding, which depends both on the repulsion between a bound toxin and a trapped cation and on the probability of cation trapping. A more general analysis would identify the experimental estimate of B_i with the average of the different tonic inhibitions due to the pore occupancy by Na^+ or Ca^{2+}, weighted by their respective probabilities (Eq. 21 of Conti et al., 1996), but this level of description is beyond the scope of this work. Equations 5 and 6, defining the parameters of TTX binding to open channels that can freely lose repelling cations, are instead totally general.

RESULTS

Tonic block

Fig. 2 illustrates the wide range of tonic TTX sensitivity of the various sodium channel phenotypes studied in this work. Each panel shows records of the sodium currents elicited by a single pulse depolarization in an oocyte expressing the indicated phenotype before and after the addition of TTX at a concentration, [T], close to the respective $\mathrm{IC}_{50}^{(t)}$. The pulse was applied under stationary conditions after a resting period at the holding potential (−100 or −120 mV) sufficient for the abolition of use-dependent effects induced by previous stimulations. The time required for UD effects to subside was tested in preliminary experiments. As expected from the theory, this time is related to the time constant of the off-binding reaction of TTX, τ_0 (see Table 1). In the experiments of Fig. 2 the resting periods were 20 s for mutant D1717Q, 1 min for W386Y and E945Q, 3 min for WT, and 6 min for D1426K. Notice that the [T] values used in the various experiments vary by more than three orders of magnitude, from 4 nM in the experiment with D1426K to 10 μM in the case of mutant D1717Q. Notice also that TTX reduces in all cases the amplitude of the response without changing appreciably its time course, as expected if only the binding to the blocking site affects the performance of the channels, whereas the interaction with other hypothetical sites does not influence channel gating.

A summary of the tonic dose-response characteristics of each phenotype, as obtained from several experiments at different [T], is given in Fig. 2 *F* as plots of the resting percentage of unblocked currents (toxin-free channels), U_0, against log([T]). The data are well fitted by the simple Michaelis-Menten relationship (Eq. 1), with $\mathrm{IC}_{50}^{(t)}$ values ranging from ~4 nM for D1426K to ~11 μM for D1717Q. The best fitting values of $\mathrm{IC}_{50}^{(t)}$ for the various phenotypes are given in the legend to Fig. 2 and in the second column of Table 1. These estimates are fairly consistent with those reported by Terlau et al. (1991). However, our data exhibit a smaller standard deviation and are free from possible systematic errors that could have affected the earlier estimates because of insufficient awareness of the detailed

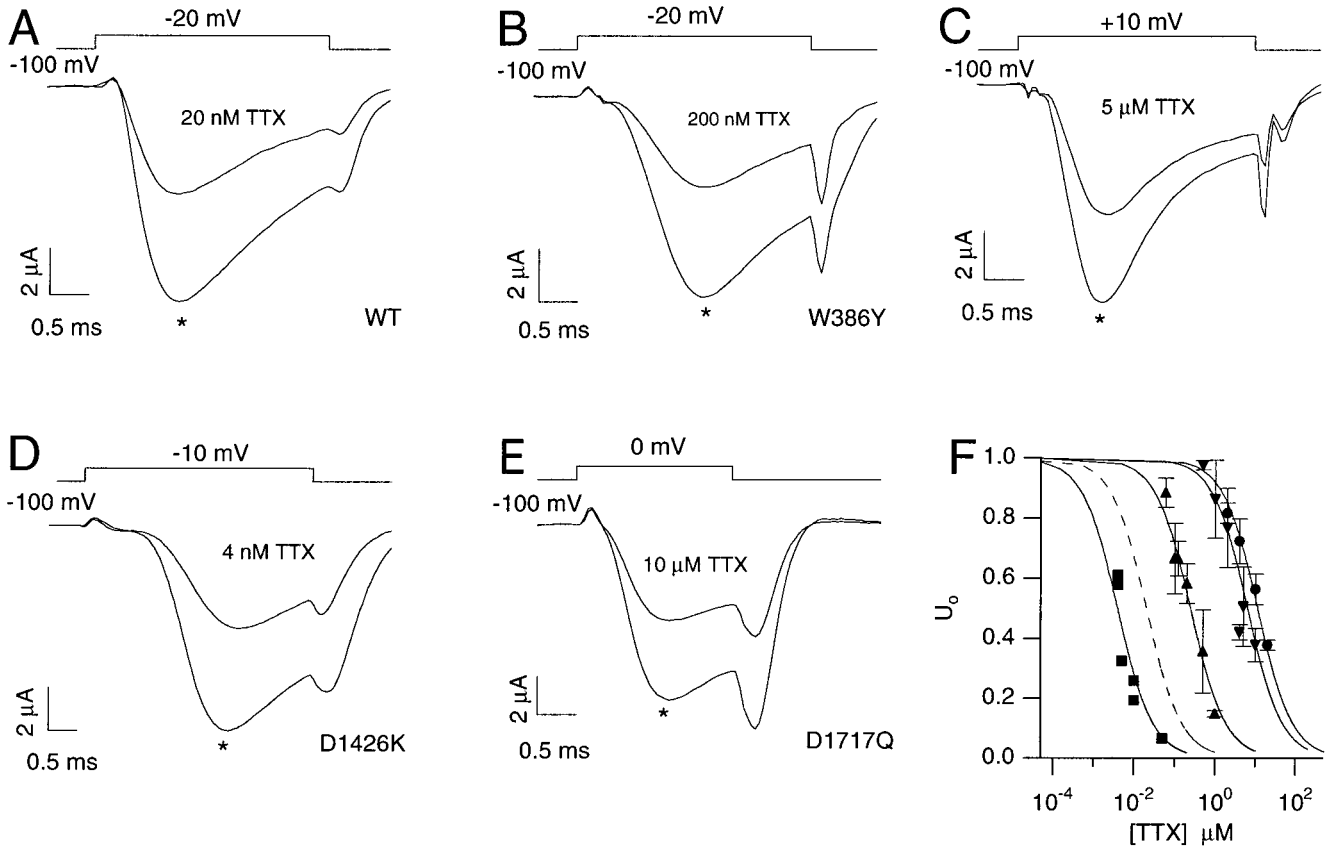

FIGURE 2 Tonic block by TTX of the sodium currents mediated by WT and mutant channels. (*A–E*) Sodium currents recorded from whole oocytes bathed in NFR before (*) and after the addition of TTX at the indicated concentrations. The responses were elicited by the depolarizing pulses indicated in the figure after long resting periods at −100 mV to allow the removal of UD effects from previous stimulations. Notice the very wide range of toxin concentrations needed to obtain similar blocking effects (40–60%) for the various phenotypes. (*F*) Dose response of the tonic TTX block of mutant channels as compared to WT (– – –). The ordinate gives the resting toxin-free probability, U_0, defined as the fraction of sodium current remaining after the addition of TTX at the concentration given on the abscissa on a logarithmic scale. Except for the D1426K data, reporting single measurements, the various symbols represent mean values (± SD) from at least three different measurements at a given [T]. ■, D1426K; ▲, W386Y; ▼, E945Q; ●, D1717Q. The smooth lines are least-squares fits with Eq. 1, yielding the estimates given in the second column of Table 1, which range from 4 nM for D1426K to 11 μM for D1717Q .

use-dependent properties of TTX block that we describe below.

Use-dependent block of D1426K, W386Y, and E945Q

Like that of WT channels, the block by TTX of the sodium currents mediated by three of the mutants studied in this work can be easily shown to have use-dependent properties. Fig. 3 shows measurements of the decay of the fraction of toxin-free channels during repetitive stimulations with short depolarizing pulses given at 0.6-s intervals. In each of the experiments illustrated in Fig. 3 an oocyte expressing WT, W386Y, D1426K, or E945Q was exposed to a TTX concentration close to the tonic $IC_{50}^{(t)}$ of each phenotype, and the train stimulation was started after a suitable resting period at a holding potential. Peak currents elicited by the various pulses of the train are normalized to those measured with

TABLE 1 Summary of the parameters characterizing the affinity and the kinetics of TTX binding to resting and stimulated sodium channel mutants

	$IC_{50}^{(t)}$ (nM)	$IC_{50}^{(s)}$ (nM)	τ_0 (s)	B_i	$k_{off}^{(0)}$* (s)	k_{on}* (μM*s)
WT*	26 ± 4	8.9 ± 1.2	53 ± 16	0.66	0.019	2.1
W386Y	247 ± 19	77 ± 5	7.2 ± 0.3	0.69	0.14	1.8
E945Q	6.3 ± 0.6 × 10^3	2.2 ± 0.2 × 10^3	12.0 ± 0.8	0.67	0.083	0.038
D1426K	3.9 ± 0.6	1.7 ± 0.3	225 ± 7	0.56	0.0044	1.9
D1717Q	11.3 ± 0.7 × 10^3	4.6 ± 0.3 × 10^3	103 ± 6 × 10^{-3}	0.60	9.71	2.1

Data are means ± standard deviation.
*The wild-type data are taken from Conti et al. (1996).

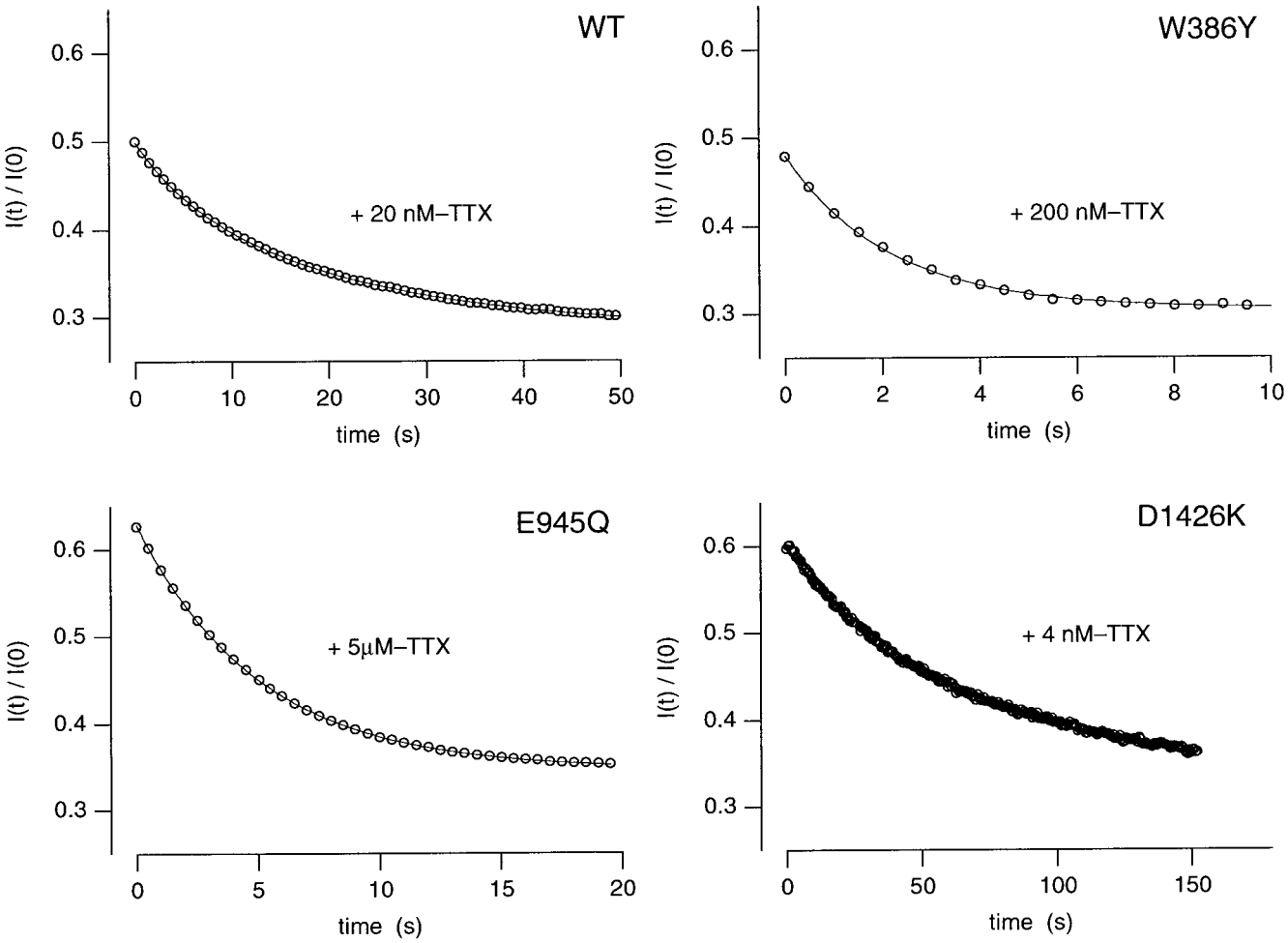

FIGURE 3 Use dependence of TTX block of mutants W386Y, E945Q, and D1426K, compared to that of the WT channel, as revealed by the response to repeated stimulations with the same short pulse at 0.6-s intervals, starting from resting conditions of ~50% tonic block. The peak responses to the various pulses are normalized to those measured with an identical protocol in toxin-free conditions and plotted as a function of time of stimulation. Notice the very different time scale of the use-dependent decays observed for the various phenotypes, as opposed to the roughly equal size of the effect. The decline of the fraction of unblocked currents is well fitted for all phenotypes by a single exponential according to Eq. 1 (*smooth lines*). The values of the parameters U_0, U_∞, and τ that best fit the data are 0.5, 0.28, and 16.3 s for WT; 0.48, 0.31, and 2.2 s for W386Y; 0.63, 0.35, and 5.1 s for E945Q; and 0.6, 0.34, and 61 s for D1426K.

the same protocol before the addition of the toxin and plotted as a function of the time elapsed from the beginning of the train stimulation. It is seen that this quantity, $U(t)$, representing the fraction of toxin-free channels, decreased with time of stimulation as a single exponential (*solid line*) according to Eq. 2.

As previously described for WT channels (Conti et al., 1996), we found for all phenotypes that the asymptotic loss of the sodium currents and the rate of their decrease increased with the frequency of stimulation, but approached finite limiting values (data not shown). The frequency of stimulation in the experiments of Fig. 3 was high enough to yield use-dependent effects close to these limits. The most interesting observation from the data of Fig. 3 is that, despite more than a 1000-fold variation in their tonic TTX sensitivity, the various phenotypes show a similar relative increase in toxin binding affinity during stimulation. In all cases the initial toxin-free probability of ~0.5 is asymptotically reduced by almost a factor of 2. Thus each particular mutation has similar effects on the binding of TTX to both resting and stimulated channels, and this strongly supports the idea that the two processes involve the same receptor site.

In contrast to the extent of cumulative extra block, the kinetics of TTX UD shows large phenotypic variations; the time constants of the exponential relaxations of Fig. 3 range from 2.2 s for mutant W386Y to 61 s for mutant D1426K. The development of cumulative extra block is due to the convolution of the effects of single pulses (Makielski et al., 1993; Conti et al., 1996). A distinctive feature of STX-and TTX-UD with respect to the phasic block of local anesthetics (Butterworth and Strichartz, 1990; Hille, 1992) is that the extra block induced by a single brief stimulus develops with a biphasic time course only after the pulse. Fig. 4 shows representative experiments illustrating this property for WT, W386Y, and E945Q. Double-pulse stimulations

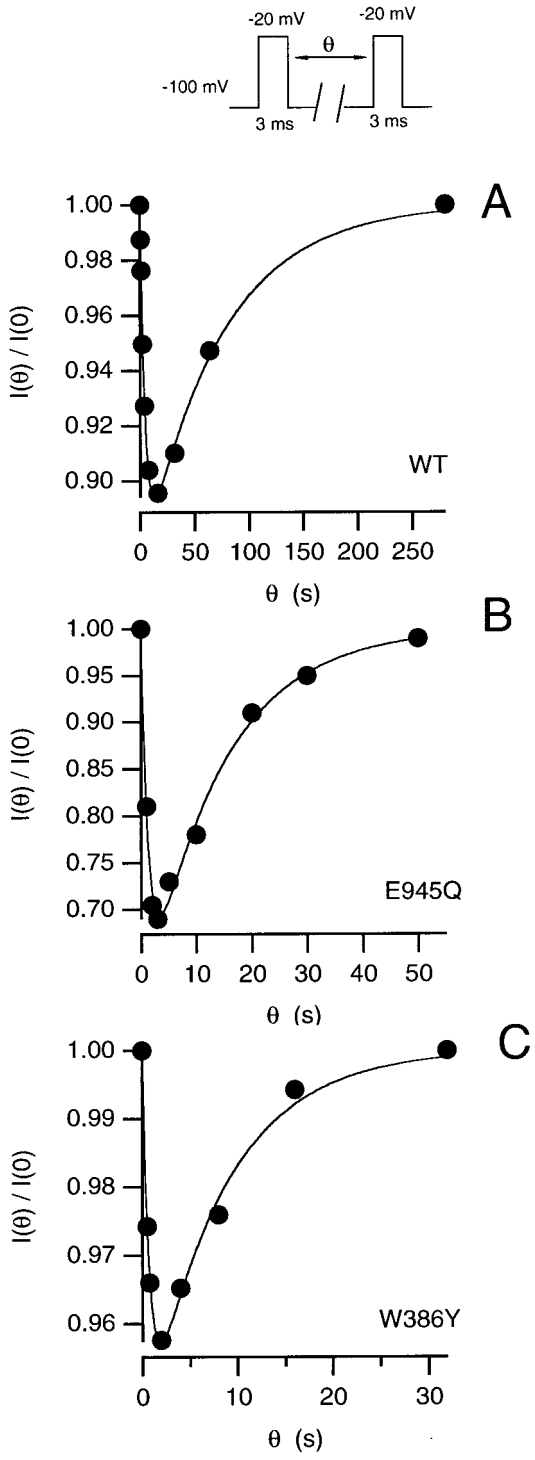

FIGURE 4 TTX block relaxations induced by a brief depolarizing pulse, as revealed by the double-pulse stimulation protocol shown in the inset. The ratio of second to first peak currents, $I(\theta)/I(0)$, is plotted as a function of the interpulse duration, θ. The data are fitted by double-exponential functions with time constants, τ_f and τ_s. (*A*) WT and 20 nM-TTX: τ_f = 4.5 s, τ_s = 70 s. (*B*) E945Q and 10 μM-TTX: τ_f = 1.3 s, τ_s = 13 s. (*C*) W386Y and 60 nM-TTX: τ_f = 0.7 s, τ_s = 7.9 s.

reveal in the response to the second pulse a transient increase of TTX block that is fairly well fitted by a double-exponential function (*solid lines*), indicating that the underlying process involves transitions between at least three states. Notice that in the various phenotypes a faster onset of cumulative extra block corresponds in general to a faster recovery from single-pulse effects.

Whereas the delayed increase in the number of blocked channels is easily explained by the finite kinetics of new TTX binding, the permanence of the higher binding affinity long enough to allow a significant extra block may have different interpretations. Various authors (Lönnendonker, 1989; Makielski et al., 1993; Satin et al., 1994) postulate that the high-affinity condition corresponds to a channel conformation that is quickly reached during activation and remains long-lived during repolarizations. According to this interpretation we would conclude that single-point mutations affect to a comparable degree both the kinetics of TTX binding and the rate of recovery of the resting channel conformation. Alternatively, the trapped-ion mechanism proposed by Salgado et al. (1986) and described by Scheme 1 explains TTX block relaxations as being due to the following sequence of events: 1) the resting distribution of the channels between toxin-free, **L**-blocked and **H**-blocked states is established by the kinetic equilibrium between the "on" and "off" rates for both types of TTX binding; 2) the conditioning pulse abruptly upsets the distribution among blocked channels (the escape of the trapped cation converts any **L**-blockade into an **H**-blockade) without changing the number of toxin-free channels; 3) whereas this leaves the TTX on binding rate unaffected, the rate of toxin dissociation immediately after the pulse (involving only more tightly bound complexes) is slower than before, when a good fraction of the blocked channels held the toxin less tightly; 4) the ensuing increase in the number of blocked channels is first damped by the relatively fast reequilibration of $\mathbf{L} \leftrightarrow \mathbf{U}$ transitions and is eventually reversed by the slower unbinding from **H**-blocked states. This mechanism predicts that both rise and decay of toxin-block relaxations depend exclusively on toxin-binding kinetics and are similarly changed by modifications of the toxin receptor site.

Measurements of single-pulse relaxations are generally less accurate than those of cumulative extra block, because the effects are much smaller and the experiments are too long (each data point requires a resting period of 1 min for E945Q and 3 min for WT; our estimate that D1426K recovers the tonic block conditions only after 6 min discouraged us from performing double-pulse measurements in this mutant). Furthermore, the dependence of the single-pulse relaxations on model parameters as described for WT channels by Conti et al. (1996) is rather involved, whereas the interpretation of cumulative extra block data in terms of relevant parameters is straightforward (see Materials and Methods, Eqs. 5–7). For these reasons our comparative study of the mutant channels was based primarily on the latter type of measurements.

The data characterizing the [T] dependence of the stimulated block for all of the phenotypes studied in this work are given in Fig. 5, including measurements on mutant D1717Q that required a more complex analysis discussed

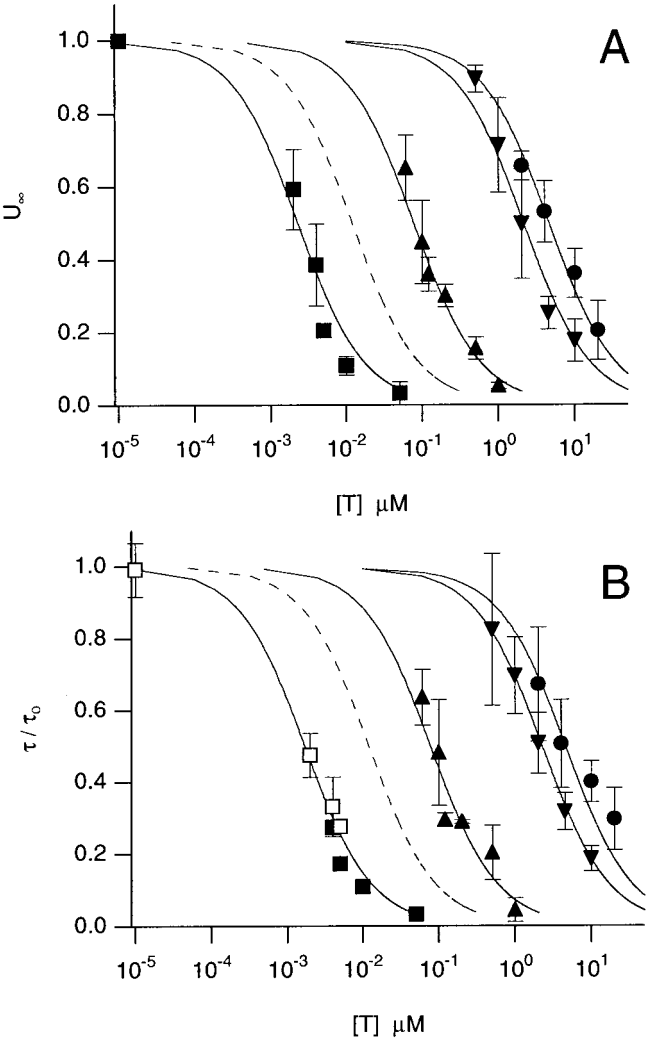

FIGURE 5 (*A*) Comparison of the dose responses for stimulated TTX block of mutant (*symbols*) and WT (*dashed line*) sodium channels. The toxin-free probability, U_∞, derived from the fitted asymptotic values during train stimulations as described in Fig. 3 is plotted against the logarithm of [T]. Data for mutant D1717Q are obtained from measurements of the type described in Fig. 7. ■, D1426K; ▲, W386Y; ▼, E945Q; ●, D1717Q. The error bars represent ± SD from at least three different measurements at a given [T]. No bar indicates a single measurement. The continuous lines are fits with Eq. 3, using the $IC_{50}^{(s)}$ values given in the third column of Table 1, ranging from 1.7 nM for D1426K to 4.6 μM for D1717Q. These are the values that yield the best fit of combined U_∞ and τ data according to Eqs. 3 and 4, with $IC_{50}^{(s)}$ and τ_0 as fitting parameters. (*B*) Similar comparison for the [T] dependence of the time constant, τ, of the stimulated decay of toxin-free probability, normalized for each phenotype, to the respective estimated upper limit, τ_0, given in the fourth column of Table 1 and ranging from 103 ms for D1717Q to 225 s for D1426K. For mutant D1426K the data include as open symbols the time constants of binding relaxations measured in wash-in/wash-out experiments. Symbols and error bars are as in *A*. Data for D1717Q are from measurements described in Fig. 7. The continuous lines are fits according to Eq. 4.

later. For mutants W386Y, D1426K, and E945Q, experiments of the type illustrated in Fig. 3 were performed at various values of [T], and $U(t)$ was fitted according to Eq. 2 to obtain estimates of U_0, U_∞, and τ. The values of U_∞ are plotted in Fig. 5 *A* versus the logarithm of [T]; they were fitted by Eq. 3 (*solid lines*) to obtain the estimates of $IC_{50}^{(t)}$ given in the figure legend and in the third column of Table 1. The dashed line represents WT data and was drawn according to the estimates given by Conti et al. (1996). Plots of the [T] dependence of τ are shown in Fig. 5 *B*. For an easier comparison, τ values for each phenotype are normalized to the respective estimate of τ_0 obtained from the least-squares fit with Eq. 4 (*solid lines*) and given in the fourth column of Table 1. It must be stressed that the same values of $IC_{50}^{(t)}$ were used for the fit of both U_∞ and τ data, in agreement with the model underlying Eqs. 3 and 4. For D1426K we have also plotted in Fig. 5 *B* (*open symbols*) the time constants of toxin binding relaxations measured from the wash-in/wash-out experiments discussed later. It is seen that these quantities are also well fitted by Eq. 4, as expected from Scheme 1. In particular, the wash-out time constant should be equal to the estimate of τ_0 derived from use-dependent relaxations, in agreement with our observations.

Wash-in/wash-out experiments

Fig. 6 *A* shows the time course of a wash-in/wash-out experiment on an oocyte expressing D1426K, the most TTX-sensitive phenotype of this study that is also characterized by the slowest TTX binding kinetics. The oocyte was kept at a holding potential of −100 mV and exposed to several long periods of repetitive pulse stimulations at 0.6-s intervals while being perfused with a constant flow of bathing solutions with [T] values that could be effectively changed within ~10 s. The upper diagram of the figure shows the time record of the peak responses measured for every applied test stimulus normalized to the mean value measured for [T] = 0, and the lower diagram shows the timing of the various switches of [T] levels. Any switch of [T] was made during continuous stimulation when the responses were fairly stationary. Switching from [T] = 0 to [T] = 2 nM caused an exponential decrease of the responses by almost a factor of 2 with a time constant of ~100 s, much larger than expected for the onset of a steady [T] value and reflecting the binding kinetics of TTX to steadily stimulated channels. By the use of Eqs. 3 and 4, these data yield for D1426K the estimates $IC_{50}^{(s)} \approx 2$ nM and $\tau_0 \approx 220$ s. A second switch of solution to [T] = 4 nM caused a further decrease of the currents toward ~30% of the toxin-free level with a time constant of ~60 s. The parameters of this second relaxation are consistent with the predictions of Eqs. 3 and 4 for [T] = 4 nM and for the same values of $IC_{50}^{(s)}$ and τ_0. The experiment proceeded by allowing a resting period of more than 5 min with [T] kept at 4 nM before starting a new stimulation epoch. The pause caused a strong reduction of TTX block: the first response after the resting period was almost doubled, as expected for an $IC_{50}^{(t)}$ of ~4 nM according to the tonic block data described in Fig. 2. However, the successive responses to the new train stimulation decayed again toward the same asymptotic level of the previous one with a time constant of ~55 s, very close to that measured

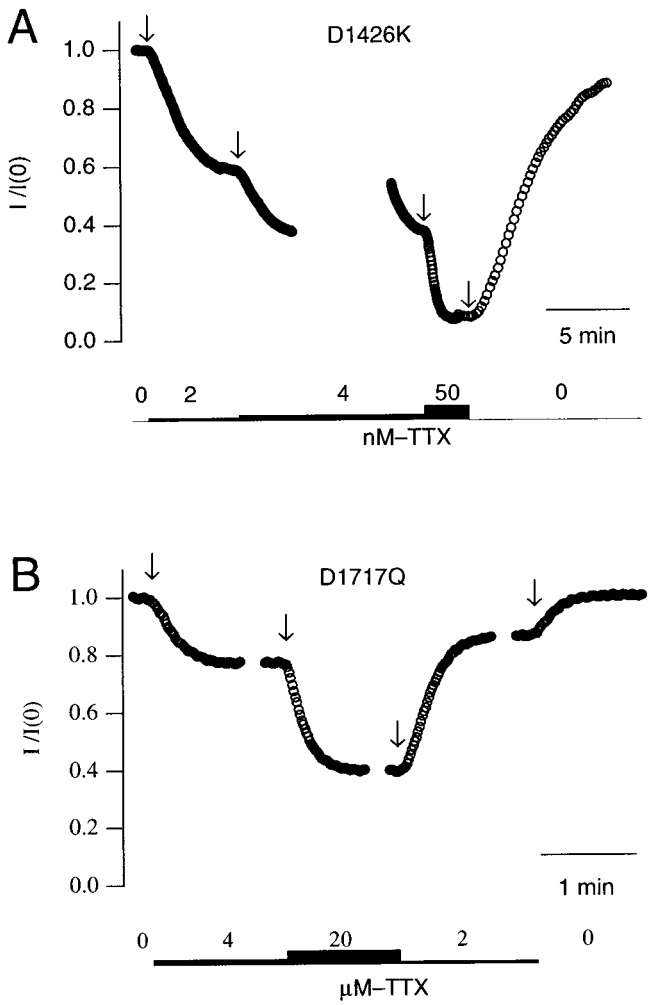

FIGURE 6 Time course of the normalized peak response of mutants D1426K (*A*) and D1717Q (*B*) to a fixed pulse stimulation during wash-in/wash-out experiments. Changes of TTX concentration, [T], produced by switching the solution feeding the continuous perfusion system, are indicated in the bottom diagram of each experiment; these required an effective settling time in the range of 10 s. (*A*) The decay of the peak currents after the addition of 2 nM TTX and the next increase of [T] to 4 nM is much slower than the change of solution. In 2 nM TTX the responses are asymptotically reduced by ~50% with a late time constant of ~100 s, and 4 nM TTX causes a further decrease to ~30% of control with a time constant of ~60 s. After a resting period of ~5 min at 4 nM TTX, the first test response to a new train stimulation is almost doubled, whereas the successive ones decay again toward the previous steady level with a time constant of ~55 s. During the next perfusion with 50 nM TTX, the sodium currents drop to ~4% with a time constant of ~20 s dominated by the perfusion system. Upon return to [T] = 0, the test responses tend to recover the control level with a time constant of ~200 s. (*B*) Similar experiment on an oocyte expressing the ~1000-fold less TTX-sensitive mutant D1717Q. Switching [T] in the sequence 0, 4 μM, 20 μM, 2 μM, and returning to 0 causes blocking and unblocking effects with the same time constant of ~12 s, governed exclusively by the timing of the perfusion system. The steady-state levels of the test responses at any [T] reflect tonic block, because use-dependent effects subside completely within the repolarization period of 0.6 s between successive test stimulations.

for the increase of stimulated block upon switching to [T] = 4 nM. A third change of solution to [T] = 50 nM reduced the sodium currents to ~4% of the toxin-free level with an apparent time constant of less than 20 s, most likely dominated by the timing of the perfusion system (see also Fig. 6 *B*). The recovery of the original control responses during perfusion with a TTX-free solution was very slow: after the first signs of recovery, the pulse-repetition interval was changed to 2 s, and the wash-out of TTX block appeared as a single exponential with a time constant of ~200 s, consistent with the above estimates of τ_0 from on binding and UD kinetics. In four different experiments of this type, the estimated wash-out time constant for TTX unblock of D1426K channels ranged between 206 and 247 s, in good agreement with the value of 225 s (Table 1), which fits the overall data of UD and wash-in kinetics according to Eq. 4.

The kinetics of TTX binding to WT channels is faster than for D1426K; the time constants estimated from use-dependent block relaxations at [T] = $IC_{50}^{(t)}$ are smaller than 20 s (Conti et al., 1996). This makes the measurement of wash-in time constants with the perfusion system used in this work unreliable. However, the wash-out time constant for TTX unblock of WT channels could be easily measured in three experiments that yielded values ranging from 50 to 62 s, in good agreement with the earlier estimate of τ_0 = 53 s by Conti et al. (1996).

Fig. 6 *B* shows a wash-in/wash-out experiment on an oocyte expressing the least TTX-sensitive mutant D1717Q, which, as discussed later, shows very fast TTX binding relaxations on a time scale of tens of milliseconds. Apart from the need to use [T] values that are three orders of magnitude higher (changed in the sequence 0, 4 μM, 20 μM, 2 μM, 0), two main features distinguish this experiment from that of Fig. 6 *A*. First, the binding and unbinding kinetics of TTX are too fast to be resolved using our slow perfusion system: all wash-in/wash-out effects developed with the same time constant of ~12 s, obviously governed exclusively by the time required for a complete change of the solution in the recording chamber. Second, there is no appreciable evidence of any use-dependent relaxation: at constant [T], repetitive pulses at 0.6-s intervals elicited practically indistinguishable responses, and resting periods of tens of seconds did not change the first response to any stimulation epoch. Evidently, any extra block possibly induced by a single pulse in mutant D1717Q develops and subsides entirely in less than 0.6 s. Indeed, we show below that use-dependent relaxations of TTX block also occur in mutant D1717Q, but they are much too fast to be seen with the relatively low frequency of stimulation used in this experiment. We conclude that the fraction of unblocked currents at any steady [T] value in the experiment of Fig. 6 *B* reflects the binding of TTX to resting channels, and data from this and similar experiments with D1717Q are accordingly plotted in Fig. 2 *F* and fitted to Eq. 1 to yield the estimate of 11.3 μM given in Table 1 for the $IC_{50}^{(t)}$ of this mutant.

Use-dependent block of mutant D1717Q

Finding a constant fraction of blocked D1717Q channels when testing with pulse depolarizations at 0.6-s intervals

does not imply that TTX binding to these channels lacks use-dependent effects; it is instead a consequence of the fact that the changes induced by each test pulse subside during the following repolarization period. Indeed, if the ~400-fold increase in the $IC_{50}^{(t)}$ of mutant D1717Q arises primarily from an increase in the rate of TTX dissociation, the relaxation time of TTX binding to D1717Q at the $IC_{50}^{(t)}$ is expected to be ~400 times shorter than the respective value for WT, falling in the range of tens of milliseconds. In this case a use-dependent increase of TTX block is observable only during repetitive stimulations at frequencies above 10 Hz.

Fig. 7 illustrates an experiment on an oocyte expressing D1717Q channels and tested with high-frequency repetitive stimulations before and after the addition to the bathing solution of 10 μM TTX. The stimulation protocol consisted of 20 identical pulses of 2 ms to 10 mV separated by a

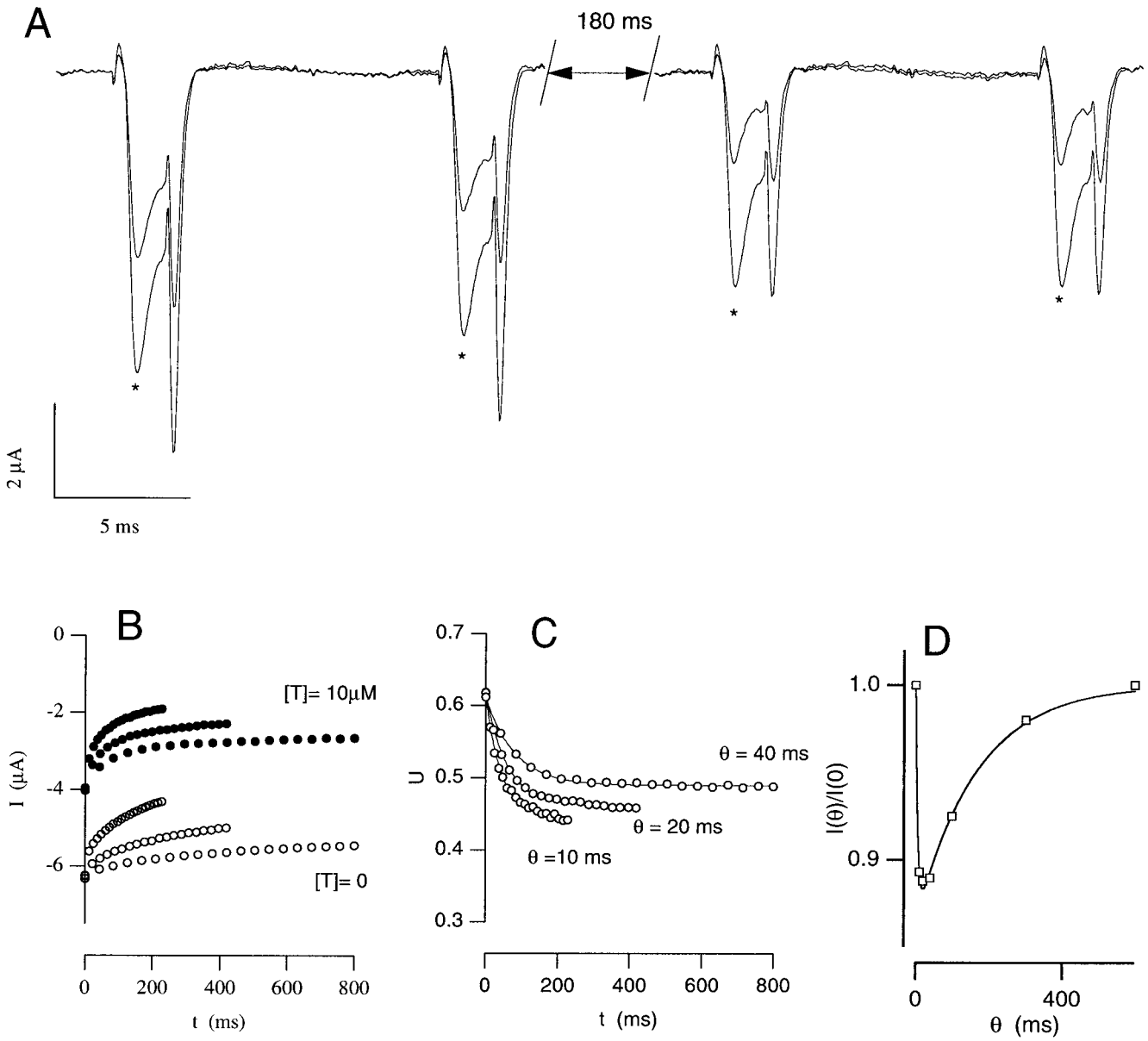

FIGURE 7 Fast use-dependent relaxations of the blockade of D1717Q channels by TTX. (*A*) Superimposed traces of the responses to a train stimulation (2-ms pulses to +10 mV with 10-ms intervals at −100 mV) recorded before and after the addition of 10 μM-TTX. Only the segments containing the first two and the last two of the 20 responses of each train are shown. In the presence of TTX, the progressive decay of the responses is much stronger than expected from the cumulative inactivation observed in toxin-free conditions. (*B*) Time course of the peak currents recorded with the same protocol, using pulse intervals, θ, of 10, 20, or 40 ms. Empty and filled circles denote, respectively, measurements in 0 and 10 μM TTX. (*C*) Decay of the block-free probability, U, estimated by the ratio of toxin to toxin-free data in *B*. The solid lines show best fits with single exponentials obtained for the following time constants and asymptotic values: 80.8 ms and 0.49 for $\theta = 40$ ms; 58.8 ms and 0.462 for $\theta = 20$ ms; 43.0 ms and 0.446 for $\theta = 10$ ms. Linear extrapolation of these values to the limit of $\theta = 0$ yields estimates of 0.43 and 32 ms for the open-channel block parameters U_∞ and τ to be used in Eqs. 3 and 4. (*D*) TTX block relaxations measured by the ratio of second to first peak currents, $I(\theta)/I(0)$, also for larger values of θ. The delayed onset of extra block is barely appreciable, because the effect is already at maximum for $\theta = 20$ ms. The solid line is a double exponential, with $\tau_f = 5.6$ ms and $\tau_s = 163$ ms.

stimulation interval, θ, of 10, 20, or 40 ms. Fig. 7 *A* shows the first two and the last two responses elicited by a train with $\vartheta = 10$ ms after and before the addition of TTX. It is seen that even in toxin-free conditions, the successive responses to such high-frequency stimulation decay asymptotically by ~30% because of cumulative inactivation. It is also apparent, however, that the percentage reduction of the currents is much stronger in the presence of 10 μM TTX, where the last peak current is only 47% of that of the first pulse. Peak currents measured in this experiment for pulse trains with $\theta = 10$, 20, or 40 ms are plotted in Fig. 7 *B* versus time from onset of the first pulse; open symbols show data before TTX addition, and filled symbols refer to measurements at [T] = 10 μM. The most obvious way to unfold TTX-induced effects from those of cumulative inactivation is to assume that the latter process affects indifferently toxin-free or toxin-blocked channels, so that the ratio of the peak currents measured with the same protocol before and after TTX addition estimates the block-free probability, $U(t)$, at the time t of the test pulse. Plots of these ratios are shown in Fig. 7 *C* for the three different stimulation frequencies. As expected, all three protocols give the same value of $U(0)$. However, the decay of $U(t)$ with time of stimulation, although always well fitted by a single exponential relaxation (*solid lines*), depends on the stimulation interval θ: both the asymptotic value and the time constant of $U(t)$ decrease with θ. As discussed in detail for WT channels by Conti et al. (1996), this result is expected from Scheme 1 if the stimulation interval is comparable with the time constant that governs the binding of TTX to open channels. UD measurements with stimulation intervals shorter than 10 ms are impractical because they would be too heavily affected by cumulative inactivation effects. Therefore, the limiting values, U_∞ and τ, to be related to open-channel block according to Eqs. 3 and 4, were estimated by linear extrapolation of the measurements of the asymptotic value and time constant of $U(t)$ at $\theta = 40$, 20, and 10 ms. Estimates of U_∞ and τ obtained from several experiments of the type illustrated above are plotted in Fig. 5 to characterize the block by TTX of open D1717Q channels. In the experiment of Fig. 7 these values were $U_\infty = 0.43$ and $\tau = 32$ ms. As for all of the other phenotypes in this study, the activated state of D1717Q channels is more than twice as sensitive to TTX block than the resting state. The major distinctive feature of D1717Q appears to be that the kinetics of TTX binding to these channels is ~500 times faster than for WT. As a further support to this conclusion, double-pulse measurements (corrected as above for normal inactivation) show that also for D1717Q the transient extra block induced by a single pulse is biexponential (Fig. 7 *D*) and differs roughly from that observed for the other phenotypes only by a mere change of time scale.

DISCUSSION

We have described in this paper measurements of equilibrium and relaxations of TTX binding to mutants of the rBIIA sodium channel with modified single residues in the outer pore region. The results of our study are summarized in Table 1, where the first two columns give our best estimates of $IC_{50}^{(t)}$ and $IC_{50}^{(s)}$, the TTX concentrations that block 50% of the channels, at rest or under saturating stimulation, respectively. Column 3 gives the estimated upper limit, τ_0, of the time constant of TTX binding relaxations induced by repetitive stimulations. For the slow mutant D1426K, consistent values of the time constants and direct estimates of τ_0 were also obtained from wash-in/wash-out experiments. We also verified that the time constant of TTX wash-out from WT channels agrees with the WT estimate of τ_0 obtained from the UD kinetics by Conti et al. (1996). It is important to stress that the operational definition of these quantities according to Eqs. 1–4 is model independent.

Despite phenotypic variations of $IC_{50}^{(t)}$ and $IC_{50}^{(s)}$ spanning three orders of magnitude, we find that the ratio of the mean estimates of these quantities varies barely significantly between 2.3 and 3.2. This result implies that tonic and phasic TTX block occur at the same site in the outer vestibule of the sodium channel, being affected to the same extent by point mutations that change toxin-receptor interactions. The same conclusion has been reached by Satin et al. (1994) for STX block from the study of a mutation that converts the cardiac toxin-resistant channel to the brain toxin-sensitive phenotype.

All of the mutants studied in this work show a use-dependent TTX block with the same qualitative features described by Conti et al. (1996) for WT channels. Quite generally, we find that cumulative extra-block data are well fitted by Eqs. 2–4, qualifying the UD process as the relaxation of a bimolecular binding reaction. Thus, independently of the mechanism by which pulse depolarizations change the affinity of the binding site, these data yield, according to Eqs. 5 and 6, direct estimates of the first-order dissociation and second-order association rate constants of TTX binding to the stimulated condition of its receptor. These estimates are given in the last two columns of Table 1, and their possible relevance for understanding the structure of the outer vestibule of the sodium pore is discussed later.

One goal of our study was to acquire additional information about the mechanism underlying the use dependence of TTX block. Our data confirm for all mutants the conclusion drawn for WT by Conti et al. (1996) about the consistency of stimulated extra block data with the trapped-ion model underlying Scheme 1. In particular, the prediction of Scheme 1 that transient extra-block relaxations and UD effects should occur on the same time scale was generally verified for a range of time scales spanning more than three orders of magnitude. Furthermore, the observation of large phenotypic changes of both equilibrium and relaxations of TTX binding is consistent with the trapped-ion mechanism, which describes both properties in terms of toxin-receptor interactions that are expected to change with mutations of the residues that shape the receptor pocket. On the other

hand, the model predicts that the ratio $IC_{50}^{(t)}/IC_{50}^{(s)}$ is mainly determined by the increased free energy of a toxin-receptor complex holding a trapped cation, possibly modulated according to Eq. 7 by the probability of cation trapping. A simple interpretation of the fair invariance of $IC_{50}^{(t)}/IC_{50}^{(s)}$ is that our mutations, although changing by several kT units the free energy of the toxin-receptor complex (e.g., an increase of $\sim 6kT$ for D1717Q relative to WT), have little influence on the distance between a bound TTX and a trapped cation and on the probability of cation occupancy of the outermost site in the conduction pore. However, this conclusion must be confirmed by studies of sodium and calcium dependence similar to those reported for WT channels (Conti et al., 1996).

As discussed by Conti et al. (1996), the transient TTX block relaxations and the cumulative UD effects predicted by Scheme 1 can be equally well described according to an alternative three-state scheme that assumes an intrinsic state dependence of TTX binding (Makielski et al., 1993). Such a scheme is representative of a class of models that postulate the existence of channel conformations with higher TTX affinity transiently visited along the channel activation pathway (Lönnendonker, 1989, 1991a,b; Eickhorn et al., 1990; Patton and Goldin, 1991; Makielski et al., 1993; Satin et al., 1994). The most distinctive feature of the model proposed by Makielski et al. (1993) concerns the interpretation of the transient extra block induced by single-pulse stimulations as being mainly governed by the return of the channels to their resting conformation. Accordingly, the model could account for our observation of a general change in the time scale of TTX block relaxations only by assuming that the mutations modify simultaneously and to a comparable degree both the kinetics of the high-affinity binding of TTX and the kinetics of the conformational transitions to and from the high-affinity state. This possibility appears quite remote in view of the absence of comparable changes in the normal gating kinetics of the mutated channels (Terlau et al., 1991; see also Fig. 2) and in view of the evidence currently available that the structures shaping the pore region are different from those responsible for channel gating (see, e.g., Kallen et al., 1994).

The phenotypic variations of the association and dissociation rate constants provide new information about the interaction of TTX with specific residues that shape the outer ion pore that may be relevant for modeling the structure of the outer pore vestibule of sodium channels. Our tonic block measurements confirm the finding by Terlau et al. (1991) that the neutralization of the negative residues E945 and D1717 in the P segment of repeat II and IV, respectively, reduces the TTX binding affinity by more than two orders of magnitude. We also verified that the mutations E387Q and M1425K, involving a net increase of one positive charge in the homologous positions of repeats I and III, have such a low TTX sensitivity as to make their further study impractical. The substitution of W386 in repeat I with another aromatic residue (Y) causes only a $\sim$10-fold reduction of TTX sensitivity, and the double charge mutation of D1426 in repeat III into a lysine has the opposite effect of decreasing $IC_{50}^{(t)}$ by about a factor of seven. From these results, Terlau et al. (1991) suggested that residues E387, E945, M1425, and D1717 are located homologously in the pore-forming domain with their side chains directed toward the outer pore vestibule, whereas next neighbors like D1426 and W386 may contribute mainly to the backbone structure of the pore vestibule with their side chains pointing away from the lumen. Recent studies of cysteine mutagenesis confirm that the residues mutated in this work contribute to the shaping of the outer pore (Yamagishi et al., 1997). However, they also show that the side chains of W386 and D1426 are exposed to the external solution and argue against a precise alignment of E945 and D1717 in the voltage drop across the pore. The mutations studied here are two to four amino acid positions away from the DEKA ring of residues that strongly influence the properties of the sodium channel selectivity filter (Heinemann et al., 1992, 1994), although the structure of this crucial part of the pore is still a controversial issue (Tsushima et al., 1997; Yamagishi et al., 1997). In any case, these mutations do not change the single-channel conductance by more than a factor of 2 (Terlau et al., 1991). This supports indirectly our simple interpretation that those mutations do not change B_i because they do not affect the properties of the outermost cation-binding site of the pore.

An important contribution of our present study is the separate determination of the two rate constants, k_{on} and $k_{off}^{(0)}$, that govern the reaction of TTX binding. The presence of toxin binding relaxations that can be driven (and measured) by electrical stimulations allowed us to measure these rate constants even when the time constant of the relaxation process was a few tens of milliseconds, as in the case of mutant D1717Q. In general, mutations involving structural changes that are perceived by the toxin only after having overcome the free energy barrier for binding to its receptor are not expected to change k_{on} while causing changes of $IC_{50}^{(t)}$ that parallel those of $k_{off}^{(0)}$. With the noticeable exception of E945Q, this appears to be the case for all other mutants for which we estimate $k_{on} \approx 2\ \mu M^{-1}\ s^{-1}$, as for the WT (Table 1). The case of E945Q, which has a low TTX sensitivity comparable to that of D1717Q (see Table 1), appears quite anomalous. The increase in both $IC_{50}^{(t)}$ and $IC_{50}^{(s)}$ by a factor of $\sim$250 in mutant E945Q is due to the combination of a modest approximately fourfold increase in $k_{off}^{(0)}$ and a much larger $\sim$60-fold decrease in k_{on}. This result has important implications for the modeling of the detailed structure of the pore outer mouth. It can be speculated that the carboxyl group of E945 is closer to the entrance to the pore vestibule than that of D1717: while proceeding along the most favorable pathway to the pore-blocking position, TTX appears to interact with (be guided by) the carboxyl group of E945 much before perceiving the influence of D1717. A similar conclusion about the position of the equivalent residue E758 in the skeletal muscle sodium channel (μ1) was reached by Dudley et al. (1995) on the basis of studies of μ-conotoxin (μ-CTX) binding kinetics that is

about five times slower than that of TTX and can be easily studied in wash-in/wash-out experiments. Also in the case of μ-CTX, the mutation E758Q causes a modest twofold increase in k_{off} and an almost 100-fold decrease in k_{on} (Dudley et al., 1995). The very different structures of TTX and μ-CTX, which share only a crucial guanidinium group, further support the idea that E945 (or E758 in μ1) plays an important role in the guidance of guanidinium toxins to the blocking site.

We thank E. Gaggero for constructing the voltage-clamp amplifier.

This work was supported by Telethon project 926.

REFERENCES

Baer, M., P. M. Best, and H. Reuter. 1976. Voltage-dependent action of tetrodotoxin in mammalian cardiac muscle. *Nature.* 263:344–345.

Butterworth, G. F., and G. R. Strichartz. 1990. Molecular mechanisms of local anesthesia: a review. *Anesthesiology.* 72:711–734.

Carmeliet, E. 1987. Voltage-dependent block by tetrodotoxin of the sodium channel in rabbit cardiac Purkinje fibbers. *Biophys. J.* 51:109–114.

Cohen, C. J., B. P. Bean, T. J. Colatsky, and R. W. Tsien. 1981. Tetrodotoxin block of sodium channels in rabbit Purkinje fibbers. Interactions between toxin binding and channel gating. *J. Gen. Physiol.* 78:383–411.

Conti, F., A. Gheri, M. Pusch, and O. Moran. 1996. Use dependence of tetrodotoxin block of sodium channels: a revival of the trapped-ion mechanism. *Biophys. J.* 71:1295–1312.

Dudley, S. C., H. Todt, G. Lipkind, and H. A. Fozzard. 1995. A μ-conotoxin-insensitive Na^+ channel mutant: possible localization of a binding site at the outer vestibule. *Biophys. J.* 69:1657–1665.

Eickhorn, R., J. Weirich, D. Hornung, and H. Antoni. 1990. Use dependence of sodium current inhibition by tetrodotoxin in rat cardiac muscle: influence of channel state. *Pflügers Arch. Eur. J. Physiol.* 416:398–405.

Goldstein, S. A. N., and C. Miller. 1993. Mechanism of charybdotoxin block of a voltage-gated K^+ channel. *Biophys. J.* 65:1613–1619.

Heinemann, S. H., T. Schlief, Y. Mori, and K. Imoto. 1994. Molecular pore structure of voltage-gates sodium and calcium channels. *Braz. J. Med. Res.* 27:2781–2802.

Heinemann, S. H., H. Terlau, W. Stühmer, K. Imoto, and S. Numa. 1992. Calcium channel characteristics conferred on the sodium channel by single mutations. *Nature.* 356:441–443.

Hille, B. 1975. The receptor for tetrodotoxin and saxitoxin. *Biophys. J.* 15:615–619.

Hille, B. 1992. Ionic Channels of Excitable Membranes. Sinauer Associates, Sunderland, MA.

Kallen, R. G., S. A. Cohen, and R. L. Barchi. 1994. Structure, function and expression of voltage-dependent sodium channels. *Mol. Neurobiol.* 7:383–428.

Kao, C. Y. 1986. Structure activity relations of tetrodotoxin, saxitoxin, and analogues. *Ann. N.Y. Acad. Sci.* 479:52–67.

Kontis, K. J., and A. L. Goldin. 1993. Site-directed mutagenesis of the putative pore region of the rat IIA sodium channel. *Mol. Pharmacol.* 43:635–644.

Lipkind, G. M., and H. A. Fozzard. 1994. A structural model of the tetrodotoxin and saxitoxin binding site of the sodium channel. *Biophys. J.* 66:1–12.

Lönnendonker, U. 1989. Use-dependent block of sodium channels in frog myelinated nerve by tetrodotoxin and saxitoxin at negative holding potentials. *Biochim. Biophys. Acta.* 985:153–160.

Lönnendonker, U. 1991a. Use-dependent block with tetrodotoxin and saxitoxin at frog Ranvier nodes. I. Intrinsic channel and toxin parameters. *Eur. Biophys. J.* 20:135–141.

Lönnendonker, U. 1991b. Use-dependent block with tetrodotoxin and saxitoxin at frog Ranvier nodes. II. Extrinsic influence of cations. *Eur. Biophys. J.* 20:143–149.

MacKinnon, R., and C. Miller. 1988. Mechanism of charybdotoxin block of the high conductance, Ca^{2+}-activated K^+ channel. *J. Gen. Physiol.* 91:335–349.

Makielski, J. C., J. Satin, and Z. Fan. 1993. Post-repolarization block of cardiac sodium channels by saxitoxin. *Biophys. J.* 65:790–798.

Narahashi, T. 1974. Chemicals as tools in the study of excitable membranes. *Physiol. Rev.* 54:813–889.

Narahashi, T., J. W. Moore, and W. R. Scott. 1964. Tetrodotoxin blockage of sodium current increase in lobster giant axon. *J. Gen. Physiol.* 47:965–974.

Noda, M., W. Suzuki, S. Numa, and W. Stühmer. 1989. A single point mutation confers tetrodotoxin and saxitoxin insensitivity on the sodium channel II. *FEBS Lett.* 259:213–216.

Patton, D. E., and A. L. Goldin. 1991. A voltage-dependent gating transition induces use-dependent block by tetrodotoxin of rat IIA sodium channels expressed in *Xenopus* oocytes. *Neuron.* 7:637–647.

Pusch, M., M. Noda, W. Stühmer, S. Numa, and F. Conti. 1991. Single point mutations of the sodium channel drastically reduce the pore permeability without preventing its gating. *Eur. Biophys. J.* 20:127–133.

Salgado, V. L., J. Z. Yeh, and T. Narahashi. 1986. Use- and voltage-dependent block of the sodium channel by saxitoxin. *Ann. N.Y. Acad. Sci.* 479:84–95.

Satin, J., J. W. Kyle, M. Chen, P. Bell, L. L. Cribbs, H. A. Fozzard, and R. B. Rogart. 1992. A mutant of TTX-resistant cardiac sodium channels with TTX-sensitive properties. *Science.* 256:1202–1205.

Satin, J., J. W. Kyle, Z. Fan, R. Rogart, H. A. Fozzard, and J. C. Makielski. 1994. Post-repolarization block of cloned sodium channels by saxitoxin. The contribution of pore-region amino-acids. *Biophys. J.* 66:1353–1363.

Stühmer, W. 1992. Electrophysiological recording of *Xenopus* oocytes. *Methods Enzymol.* 207:319–339.

Terlau, H., S. H. Heinemann, W. Stühmer, M. Pusch, F. Conti, K. Imoto, and S. Numa. 1991. Mapping the site of block by tetrodotoxin and saxitoxin of sodium channels II. *FEBS Lett.* 293:93–96.

Tsushima, R. G., R. A. Li, and P. H. Backx. 1997. Altered ionic selectivity of the sodium channel revealed by cysteine mutations within the pore. *J. Gen. Physiol.* 109:463–475.

Yamagishi, T., M. Janecki, E. Marban, and G. F. Tomaselli. 1997. Topology of the P segments in the sodium channel pore revealed by cysteine mutagenesis. *Biophys. J.* 73:195–204.